

A semi-flexible aminotriazine-based
bis-methylpyridine ligand for the design of
nickel(II) spin clusters†Cite this: *Dalton Trans.*, 2014, **43**,
3044Received 15th October 2013,
Accepted 30th October 2013

DOI: 10.1039/c3dt52903g

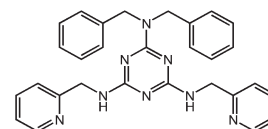
www.rsc.org/dalton

Yen-Wen Tzeng,^a Chang-Jui Lin,^a Motohiro Nakano,^b Chen-I Yang,^{*a}
Wun-Long Wan^c and Long-Li Lai^{*c}

The self-assembly of a semi-flexible aminotriazine-based bis-methylpyridine ligand, N^2,N^2 -dibenzyl- N^4,N^6 -di(pyridylmethyl)-1,3,5-triazine-2,4,6-triamine (H_2L), with $NiCl_2$ and $NiBr_2$ afforded two new nickel(II) clusters, $(H_2NMe_2)_2[Ni_5(OH)_2(H_2L)_2Cl_{10}]$ (**1**) and $[Ni_6(OH)_2(H_2L)_2Br_{10}(THF)_2]$ (**2**) showing a high spin ground state of $S = 3$.

The development of new molecule-based magnets is an important research topic in the fields of chemistry and physics, due to their impressive structural diversity and intriguing physical properties as well as complicated magneto-structural correlations.¹ One of the major challenges in the area of molecular magnetism is the construction of a polynuclear metal cluster that exhibits interesting magnetic properties, such as the high-spin ground state and/or single-molecule magnet (SMM) behavior.^{2–5} For the preparation of such metal clusters, using a polychelating ligand with an unused arm or a donor site has been recognized.^{6,7} An alternative preparation method is to utilize the flexidentate behavior of a multidentate ligand and judicious choice of bridging ligands, such as carboxylate and azide.^{8,9} Among the bridging ligands, halide ions have been known for their versatile bridging coordination modes that generate polymeric compounds.¹⁰

Poly-pyridyl ligands had a major impact in the field of supramolecular chemistry for decades, which have led to a variety of metal/ligand supramolecular ensembles to be obtained such as double and triple helices, grids, ladders, and so forth.¹¹ However, the flexible poly-pyridyl ligands are rarely exploited in the formation of polynuclear metal clusters;

Scheme 1 Schematic representation of H_2L ligand.

especially the resulting structures may potentially exhibit interesting magnetic properties.

We herein report the self-assembly of two Ni(II) clusters, $(H_2NMe_2)_2[Ni_5(OH)_2(H_2L)_2Cl_{10}]$ (**1**) and $[Ni_6(OH)_2(H_2L)_2Br_{10}(THF)_2]$ (**2**), using a semi-flexible aminotriazine-based bis-methylpyridine ligand, N^2,N^2 -dibenzyl- N^4,N^6 -di(pyridylmethyl)-1,3,5-triazine-2,4,6-triamine (H_2L). The designed ligand, H_2L (Scheme 1), contains an aminotriazine ring and two flexible methylpyridine arms, which could chelate metal ions into clusters **1** and **2**, exhibiting an $S = 3$ spin ground state arising from the uncanceled spin arrangement of the antiferro- and ferromagnetic interactions in **1** and ferromagnetic interaction in **2**, respectively.

X-ray crystal structure analysis showed that **1** and **2**† crystallize in the monoclinic space groups $P2_1/n$ and in the triclinic space groups $P\bar{1}$, respectively. In complex **1**, the geometry of the centrosymmetric Ni^{II}_5 cluster can be described as two corner-sharing μ_3 -OH-centred Ni^{II}_3 triangles with bowtie topology (Fig. 1). Two H_2L groups connect the central Ni^{II} atom (Ni1) and two peripheral metal ions in the two sides of a bow tie (Ni2 and Ni3) in a μ_3 - H_2L - κ^5 - $N,N':N''':N''''$ coordination mode, in which two methylpyridine groups exhibit in a *trans*-conformation. The base (Ni2...Ni3) of each triangle is bridged by two μ_2 - Cl^- anions. The μ_3 -OH⁻ group links the central Ni1 to the two peripheral metal ions on either side of the molecule and the O atom of OH⁻ lie out of the plane of the Ni_3 triangle about 0.402 Å. Peripheral ligations around each Ni centers are completed by terminal Cl^- anions.

The structure of complex **2** reveals a dimer of $[Ni^{II}_3(\mu_3-OH)-(\mu_3-Br)(\mu_2-Br)_3]^+$ core which is connected by two bis-chelating H_2L ligands (Fig. 2). The structure $[Ni^{II}_3(\mu_3-OH)(\mu_3-Br)(\mu_2-Br)_3]^+$ adopts a near-equilateral Ni^{II}_3 triangle core, which is bonded

^aDepartment of Chemistry, Tunghai University, Taichung 407, Taiwan.

E-mail: ciyang@thu.edu.tw; Fax: +886-4-23590426

^bDivision of Applied Chemistry, Graduate School of Engineering, Osaka University, 2-1 Yamada-oka, Suita, 565-0871, Japan^cDepartment of Applied Chemistry, National Chi Nan University, Nantou 545, Taiwan. E-mail: lilai@ncnu.edu.tw

†Electronic supplementary information (ESI) available: Detailed experimental procedures, additional crystallographic diagrams and magnetic diagram. CCDC 947250 and 947251. For ESI and crystallographic data in CIF or other electronic format see DOI: 10.1039/c3dt52903g



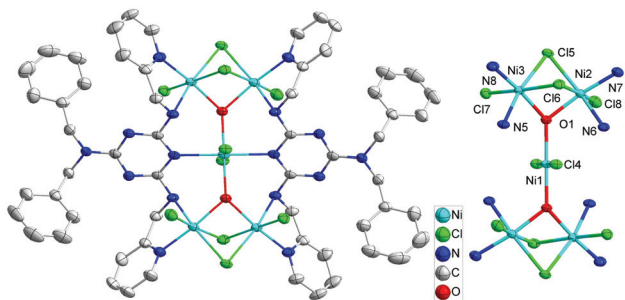


Fig. 1 Crystal structure of the anion complex **1** (left) and its Ni^{II}_5 core structure (right). The Me_2NH_2 cations and H atoms were omitted for clarity.

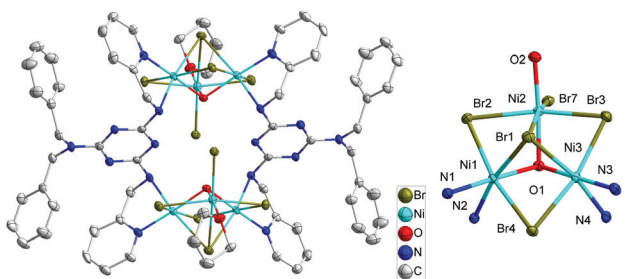


Fig. 2 Crystal structure of the complex **2** (left) and its Ni^{II}_3 core structure (right). The H atoms were omitted for clarity.

by a μ_3 -oxide (O1) and a μ_3 - Br^- (Br1) on both sides of the central planar where the central OH^- and Br^- bridges are located 0.902 and 2.056 Å above the Ni_3 plane. Each base of the Ni^{II}_3 triangle is connected by μ_2 - Br^- anions (Br2–Br4). Two H_2L ligands in complex **2** exhibit a μ_2 - $\text{H}_2\text{L}-\kappa^4-N_1N':N'',N'''$ coordination mode with *trans*-conformation of their two methylpyridine groups and connects the two Ni_3 triangles into a hexanuclear dimer of Ni_3 structure. Peripheral ligations around each Ni2 centers are ended by one terminal Br^- anion and one THF molecule.

The solid-state, variable-temperature magnetic susceptibility measurements were performed on microcrystalline samples of complexes **1** and **2** in the 2–300 K range in a 1 kOe magnetic field, which was suspended in eicosane to prevent torquing.

For complex **1**, the $\chi_{\text{M}}T$ value of $6.01 \text{ cm}^3 \text{ K mol}^{-1}$ at 300 K decreases gradually with decreasing temperature in the range of 300 to 70 K, then abruptly increases, reaching a maximum of $7.05 \text{ cm}^3 \text{ K mol}^{-1}$ at 10 K, and decreases to $4.38 \text{ cm}^3 \text{ K mol}^{-1}$ at 2 K (Fig. 3). The change in $\chi_{\text{M}}T$ value indicates that antiferromagnetic dominated in the Ni_5 unit with a non-canceled spin ground state and the $\chi_{\text{M}}T$ value at 10 K is consistent with $S = 3$ ($g = 2.2$). Below 10 K, the $\chi_{\text{M}}T$ values slowly decrease, probably due to weak intermolecular antiferromagnetic interactions, zero field splitting and/or small anisotropy.

In order to understand the magnetic coupling of complex **1**, the magnetic susceptibility data were fitted using a Ni^{II}_5 Heisenberg–van Vleck model. Based on the structure analysis, the number of magnetic interactions can be reduced significantly: J_1 for $\text{Ni}^{\text{II}} \cdots \text{Ni}^{\text{II}}$ through one μ_3 -OH and one H_2L

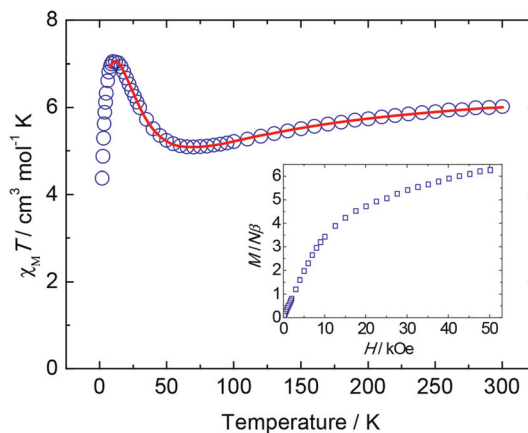


Fig. 3 Plots of $\chi_{\text{M}}T$ versus T for **1** in an applied field of 1 kOe from 2.0 to 300 K. The solid line represents a least-squares fit of the data (see text). The inset shows a 2 K magnetization isotherm collected between 0 and 50 kOe.

bridgings and J_2 for $\text{Ni}^{\text{II}} \cdots \text{Ni}^{\text{II}}$ through one μ_3 - OH^- and two μ_2 - Cl^- bridges (see Fig. S5 in the ESI †), hence the Hamiltonian can be written as:

$$H = -2J_1(S_1S_2 + S_1S_3 + S_1S_4 + S_1S_5) - 2J_2(S_2S_3 + S_4S_5)$$

The $\chi_{\text{M}}T$ data could be well fitted by this Heisenberg–van Vleck model with the addition of an intermolecular interaction by the mean-field approximation (zJ'). The results from fitting the experimental data are shown as solid lines in Fig. 3, with final parameters being $g = 2.30$, $J_1 = -11.7 \text{ cm}^{-1}$, $J_2 = 3.5 \text{ cm}^{-1}$ and $zJ' = -0.10 \text{ cm}^{-1}$. This set of parameters leads to the conclusion that the ground state is $S_{\text{T}} = 3$ and the first excited state is $S = 2$ at 24 cm^{-1} above the ground state (Fig. S6 †). The estimated values, for the intracluster magnetic exchange interactions, indicate that the antiferro- and ferromagnetic interactions are provided within the Ni^{II}_5 cluster in **1**, and are associated with an $S = 3$ spin ground state. Both interactions (J_1 and J_2) are close to the reported exchange interactions of $\text{Ni}^{\text{II}} \cdots \text{Ni}^{\text{II}}$ through the similar pathways.¹² The magnetization curve recorded at 2 K of complex **1** shows a continuous increase up to the saturation value of $6.3N\beta$ (Fig. 3 inset), which corresponds well to a ground-state spin $S = 3$, in agreement with the $\chi_{\text{M}}T$ data. However, this magnetization curve cannot be nicely fitted by the Brillouin equation for $S = 3$, probably due to the presence of intermolecular interaction, zero field splitting and/or anisotropy.

For complex **2**, the value of $\chi_{\text{M}}T$ increases steadily from $4.24 \text{ cm}^3 \text{ mol}^{-1} \text{ K}$ at 300 K as the temperature decreases to reach a maximum of $6.03 \text{ cm}^3 \text{ mol}^{-1} \text{ K}$ at 18 K, and then decreases to $1.00 \text{ cm}^3 \text{ mol}^{-1} \text{ K}$ at 2.0 K (Fig. 4). The $\chi_{\text{M}}T$ value at 300 K is slightly larger than $4.00 \text{ cm}^3 \text{ mol}^{-1} \text{ K}$, the expected value for a Ni^{II}_3 complex with noninteracting metal centers with $g = 2.3$. This behavior clearly indicates the ferromagnetic coupling within complex **2** and the decrease in $\chi_{\text{M}}T$ at low temperature (<28 K) is likely due to the intermolecular ($\text{Ni}_3 \cdots \text{Ni}_3$) interaction, the Zeeman effect or zero-field splitting



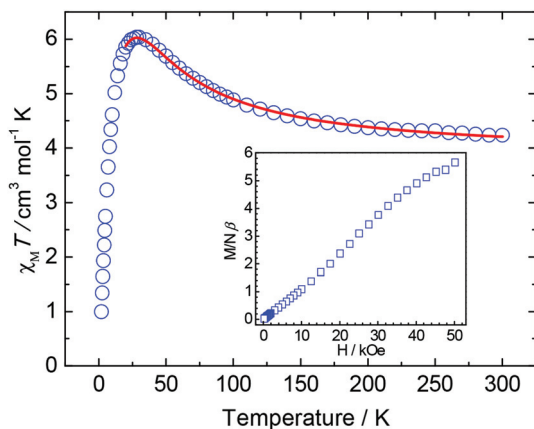


Fig. 4 Plots of $\chi_M T$ versus T for **2** in an applied field of 1 kOe from 2.0 to 300 K. The solid line represents a least-squares fit of the data (see text). The inset shows a 2 K magnetization isotherm collected between 0 and 50 kOe.

in the ground state. In order to describe the coupling within the cluster, the magnetic susceptibility data were fitted using a Ni^{II}_3 Heisenberg–van Vleck model: $H = -2J(S_1S_2 + S_2S_3 + S_1S_3)$ with an interunit interaction by the mean-field approximation (zJ') (Fig. S7†). The data below 20 K were omitted in the fitting, because zero-field splitting and Zeeman effect likely dominate in this temperature range. The fitting result of dc data in 1 kOe gave the best fit parameters of $g = 2.26$, $J = 8.10 \text{ cm}^{-1}$ and $zJ' = -0.50 \text{ cm}^{-1}$. This set of parameters gives the ground state of $S_T = 3$ and the first excited state $S = 2$ at -48 cm^{-1} above the ground state (Fig. S8†). Although the magnetic interaction between Ni^{II} ions through such bridges (one $\mu_3\text{-OH}$, one $\mu_3\text{-Br}$ and one $\mu_2\text{-Br}$) has not been reported in the literature, it is believed that the ferromagnetic interactions ensue from 6-coordinate geometry and the Ni–X–Ni bridging angles close to 90° .¹³ The magnetization curve recorded at 2 K of **2** is shown in Fig. 4 inset, in which the magnetization slowly increases with the increase of field and becomes saturated around 50 kOe with a value of $5.65N\beta$. The less rapid saturation of magnetization at low field may result from the anti-ferromagnetic interaction of $\text{Ni}_3\cdots\text{Ni}_3$ interunit and the saturation magnetization value corresponds well to a ground-state spin $S = 3$, in agreement with the $\chi_M T$ data. Again, this magnetization curve cannot be well fitted by the Brillouin equation for $S = 3$, due to the presence of intermolecular interaction and/or zero field splitting.

To investigate whether **1** and **2** might be a SMM, ac susceptibility measurements were performed with a zero applied dc field. Representative results for **1** and **2** are shown in Fig. S9 and S10.† At lower temperatures, the in-phase signal ($\chi_M''T$) increases to ~ 6.8 and $6.5 \text{ cm}^3 \text{ K mol}^{-1}$ for **1** and **2**, respectively, confirming the spin ground state of $S = 3$ for both complexes. For complex **1**, a weak χ_M'' signal appears below 5 K, which is indicative of a slow magnetic relaxation within **1**. However, the peak maxima clearly lie in the temperatures below 1.8 K, the operating limit of our instrument. These data thus suggest that compound **1** indeed exhibits a slow magnetic relaxation

or long-range magnetic ordering at temperatures below 1.8 K. In contrast, the complex **2** shows no SMM behavior from the absence of χ_M'' signal.

In conclusion, the use of semi-flexible aminotriazine-based bis-methylpyridine ligands (H_2L) has allowed the access of two novel Ni clusters with interesting magnetic properties. The H_2L ligand represents a ‘proof of feasibility’ for the belief that such ligands may provide a rich source of new transition-metal clusters. Further studies are in progress.

Notes and references

† The complexes analyzed as (C, H, N) **1**, calcd (found): C, 42.52 (42.17); H, 4.26 (4.79); N, 14.40 (14.35)% and **2**, calcd (found): C, 34.37 (34.03); H, 3.23 (3.34); N, 9.72 (9.72)%. Crystal-structure data for **1**, $\text{C}_{62}\text{H}_{70}\text{Cl}_{10}\text{N}_{18}\text{Ni}_3\text{O}_2$, $M = 1747.31$, monoclinic, $P2_1/n$, $a = 15.7038(12) \text{ \AA}$, $b = 9.9564(7) \text{ \AA}$, $c = 23.8274(18) \text{ \AA}$, $\beta = 93.4680(10)^\circ$, $V = 3718.7(5) \text{ \AA}^3$, $T = 150(2) \text{ K}$, $Z = 2$. ($R_{\text{int}} = 0.0426$), 8215 parameters, $R(R_w) = 0.0382(0.0865)$ with [$I > 2\sigma(I)$] and for **2**, $\text{C}_{66}\text{H}_{74}\text{Br}_{10}\text{N}_{16}\text{Ni}_6\text{O}_4$, $M = 2306.56$, triclinic, $P1$, $a = 11.9623(7) \text{ \AA}$, $b = 13.3874(8) \text{ \AA}$, $c = 14.2964(9) \text{ \AA}$, $\alpha = 65.3520(10)^\circ$, $\beta = 72.9400(10)^\circ$, $\gamma = 75.1400(10)^\circ$, $V = 1965.5(2) \text{ \AA}^3$, $T = 150(2) \text{ K}$, $Z = 1$. ($R_{\text{int}} = 0.0291$), 9051 parameters, $R(R_w) = 0.0256(0.0481)$ with [$I > 2\sigma(I)$].

- Magnetism: Molecules to Materials*, ed. J. S. Miller and M. Drillon, Wiley-VCH, Weinheim, Germany, 2001–2004, vol. I–V.
- (a) G. Christou, D. Gatteschi, D. N. Hendrickson and R. Sessoli, *MRS Bull.*, 2000, **25**, 66–71; (b) R. Sessoli, H.-L. Tsai, A. R. Schake, S. Wang, J. B. Vincent, K. Folting, D. Gatteschi, G. Christou and D. N. Hendrickson, *J. Am. Chem. Soc.*, 1993, **115**, 1804–1816; (c) A. Caneschi, D. Gatteschi, R. Sessoli, A. L. Barra, L. C. Brunel and M. Guillot, *J. Am. Chem. Soc.*, 1991, **113**, 5873–5874; (d) M. Nakano and H. Oshio, *Chem. Soc. Rev.*, 2011, **40**, 3239–3248.
- (a) R. Sessoli, D. Gatteschi, A. Caneschi and M. A. Novak, *Nature*, 1993, **365**, 141–143; (b) D. Gatteschi, R. Sessoli and A. Cornia, *Chem. Commun.*, 2000, 725–732; (c) Z. Sun, C. M. Grant, S. L. Castro, D. N. Hendrickson and G. Christou, *Chem. Commun.*, 1998, 721–722; (d) E. C. Yang, D. N. Hendrickson, W. Wernsdorfer, M. Nakano, L. N. Zakharov, R. D. Sommer, A. L. Rheingold, M. Ledezma-Gairaud and G. Christou, *J. Appl. Phys.*, 2002, **91**, 7382–7384; (e) C.-I. Yang, W. Wernsdorfer, Y.-J. Tsai, G. Chung, T.-S. Kuo, G.-H. Lee, M. Shieh and H.-L. Tsai, *Inorg. Chem.*, 2008, **47**, 1925–1939.
- (a) G. Christou, *Polyhedron*, 2005, **24**, 2065–2075; (b) D. Gatteschi, R. Sessoli and J. Villain, *Molecular Nanomagnets*, Oxford University Press, New York, 2006; (c) G. Aromí and E. K. Brechin, *Struct. Bonding*, 2006, **122**, 1 and references therein.
- (a) T. N. Nguyen, W. Wernsdorfer, K. A. Abboud and G. Christou, *J. Am. Chem. Soc.*, 2011, **133**, 20688–20691; (b) A. Saha, K. A. Abboud and G. Christou, *Inorg. Chem.*, 2011, **50**, 12774–12784; (c) Z. Wang, J. Van Tol, T. Taguchi, M. R. Daniels, G. Christou and N. S. Dalal, *J. Am. Chem. Soc.*, 2011, **133**, 17586–17589.



- 6 (a) A. M. Ako, I. J. Hewitt, V. Mereacre, R. Clérac, W. Wernsdorfer, C. E. Anson and A. K. Powell, *Angew. Chem., Int. Ed.*, 2006, **45**, 4926–4929; (b) S. S. Tandon, S. D. Bunge, J. Sanchiz and L. K. Thompson, *Inorg. Chem.*, 2012, **51**, 3270–3282; (c) Z. E. Serna, M. K. Urriaga, M. G. Barandika, R. Cortés, S. Martin, L. Lezama, M. I. Arriortua and T. Rojo, *Inorg. Chem.*, 2001, **40**, 4550–4555.
- 7 (a) E. E. Moushi, C. Lampropoulos, W. Wernsdorfer, V. Nastopoulos, G. Christou and A. J. Tasiopoulos, *J. Am. Chem. Soc.*, 2010, **132**, 16146–16155; (b) C. C. Stoumpos, O. Roubeau, G. Aromi, A. J. Tasiopoulos, V. Nastopoulos, A. Escuer and S. P. Perlepes, *Inorg. Chem.*, 2010, **49**, 359–361; (c) M. Murugesu, J. Raftery, W. Wernsdorfer, G. Christou and E. K. Brechin, *Inorg. Chem.*, 2004, **43**, 4203–4209; (d) T. C. Stamatatos, C. G. Efthymiou, C. C. Stoumpos and S. P. Perlepes, *Eur. J. Inorg. Chem.*, 2009, **2009**, 3361–3391.
- 8 (a) C. Papatrifaftyllopoulou, T. C. Stamatatos, W. Wernsdorfer, S. J. Teat, A. J. Tasiopoulos, A. Escuer and S. P. Perlepes, *Inorg. Chem.*, 2010, **49**, 10486–10474; (b) M. Murugesu, M. Habrych, W. Wernsdorfer, K. A. Abboud and G. Christou, *J. Am. Chem. Soc.*, 2004, **126**, 4766–4767; (c) T. C. Stamatatos and G. Christou, *Inorg. Chem.*, 2009, **48**, 3308–3322.
- 9 (a) G. Aromi, M. J. Knapp, J.-P. Claude, J. C. Huffman, D. N. Hendrickson and G. Christou, *J. Am. Chem. Soc.*, 1999, **121**, 5489–5499; (b) M. Charalambous, E. E. Moushi, C. Papatrifaftyllopoulou, W. Wernsdorfer, V. Nastopoulos, G. Christou and A. J. Tasiopoulos, *Chem. Commun.*, 2012, **48**, 5410–5412; (c) J. Esteban, L. Alcázar, M. Torres-Molina, M. Monfort, M. Font-Bardia and A. Escuer, *Inorg. Chem.*, 2012, **51**, 5503–5505.
- 10 (a) J.-M. Lehn, *Supramolecular Chemistry*, Wiley-VCH, New York, 1995; (b) C. Piguet, G. Berardinelli and G. Hopfgartner, *Chem. Rev.*, 1997, **97**, 2005–2062; (c) M. Albrecht, *Chem. Rev.*, 2001, **101**, 3457–3498.
- 11 (a) J. Esteban, P. E. Ruiz, D. M. Font-Bardia, D. T. Calvet and A. Escuer, *Chem.–Eur. J.*, 2012, **18**, 3637–3648; (b) P. L. Pawlak, A. Y. S. Malkhasian, B. Sjlivic, M. J. Tiza, B. E. Kucera, R. Loloee and F. A. Chavez, *Inorg. Chem. Commun.*, 2008, **11**, 1023–1026.
- 12 G. N. Newton, H. Sato, T. Shiga and H. Oshio, *Dalton Trans.*, 2013, **42**, 6701–6704.
- 13 A. Bencini and D. Gatteschi, *Inorg. Chim. Acta*, 1978, **31**, 11.

